EXPERIMENTAL STUDY OF A VERY LARGE FLOATING STRUCTURE EQUIPPED WITH OSCILLATING WATER COLUMN DEVICES AS MOTION ATTENUATORS

Ilaria Crema[1] and Lorenzo Cappietti[2]

Abstract: This paper presents the results of an experimental study based on small-scale physical modelling for assessing the effect of Oscillating Water Column devices (OWCs), integrated in a pontoon-type Very Large Floating Structure (VLFS), in terms of motion attenuation. The sensitivity of the VLFS length and three OWC design parameters, i.e., those most affecting the oscillating water column behaviour, has been tested, namely: the size of the chamber, the lip draught and the pressure drop induced by the orifice that connects the interior of the chamber with the external atmospheric pressure.

INTRODUCTION

The increasing population density will have a relevant impact on the limited availability of land in coastal areas of some world regions. In this context, Very Large Floating Structures (VLFS), i.e. floating structures characterized by sizes greater than the characteristic wave length of a given sea site, might represent an alternative to the commonly adopted land reclamation approach for creating usable spaces (Wang & Tay, 2011).

At the same time, the shortage of fossil fuels and the pollution problems related to their use are stimulating the transition toward the renewable energies such as the wave energy. In this context, the Oscillating Water Column (OWC) is a well know concept for exploitation of the wave energy (Falcao, 2010). In its basic form, an OWC is a hollow caisson partially immerged below the sea surface thus creating a column of water and a volume of air above it constrained within its walls. The incident waves excite the internal water column that in turn compresses and decompresses the air volume thus producing an airflow through a duct. However, if a self-rectifying air turbine is used, to transform the oscillating air flows in a unidirectional rotational motion, it can activate an electrical generator thus transforming the absorbed energy in a usable form. Because of this process, the energy of the wave is absorbed and dissipated as air flows and it is why the OWC has been proposed as shore defence structure (Boccotti, 2003). He et al. (2012) and He et al. (2013) presented an experimental study of OWCs integrated in floating breakwaters, as a sustainable option for cost sharing between wave energy capturing devices and shore protection structures. They also showed the insignificant effect of the OWC draught on the amplitude of the heave response at its natural period.

1 Department of Civil and Environmental Engineering, University of Florence, (Italy). Email: ilaria.crema@dicea.unifi.it

2 Department of Civil and Environmental Engineering, University of Florence, (Italy). Email: lorenzo.cappietti@unifi.it

Furthermore, the OWC is also counted in the literature as a possible device that may control the behaviour of VLFS (Wang et al., 2010) or floating breakwaters (He et al. 2012 and He et al. 2013).

Generally, the OWC absorbs part of the incident energy that is thus subtracted to the total amount of energy that excites the VLFS or the floating breakwater motion. It is hence motivated the development of a VLFS equipped with OWC devices for exploiting the wave energy and attenuate the motion of the floating structure.

Wang et al. (2010) reported a literature review on the several methods proposed to minimize the VLFS floating response under wave action such as breakwaters, submerged plates, OWC breakwaters, air-cushion, auxiliary attachments and mechanical joints.

Maeda et al. (2000) and Maeda et al. (2001), Ikoma et al. (2003), Hong and Kyoung (2006), Hong and Kyoung (2007), Kyoung and Hong (2008) and Hong et al. (2009) proposed an OWC anti-motion device attached to the fore-end of the VLFS.

Shigemitsu et al. (2001), investigated the floating response of the Mega-Float attached with the three-continuous OWC anti-motion devices.

In this paper, the effectiveness of an OWC in attenuating the motion of a VLFS is investigated by means of an experimental study based on small-scale physical modelling.

EXPERIMENTAL METHODOLOGY

A small-scale physical model of a VLFS was built and its floating behaviour, under the action of regular and irregular waves, was measured by testing this model in a wave-current flume. The assessment of the effects of OWCs in attenuating the VLFS motion has been based on the comparison between the measurements collected during tests where the VLFS was not equipped with OWCs and tests where the OWCs were attached to it.

The VLFS-OWC model

To reproduce properly the VLFS-OWC system, considering the predominance of gravitational forces among those related to the viscosity, the surface tension, the roughness, etc. (Huges, 1993), the scale model was designed according to the Froude similarity, with a scale factor 1:50.

The VLFS model was manufactured by assembling several hollow modules made with methacrylate panels. Each module was 0.60m wide, 0.45m high and 0.20m deep along the wave propagation direction. A valve was installed in the roof of each module to fill in or out the air inside the air cushion over which the module float thus imposing the target freeboard. Four stainless steel wire ropes, installed two by two along each VLFS side and fixed at the leading and back edges, were properly pre-tensioned to hold together all the units and to control the flexibility to the VLFS model (Fig. 1).

The OWC model was built as a rectangular-shaped box made of methacrylate and the OWC chamber was made water- and airtight by using silicone as sealing. An orifice located on the centre of the top cover assured a quadratic relation between the pressure drop and the air discharge that flows through the orifice. In fact, an orifice mimics the presence of the self-rectifying impulse air turbines, often proposed as

Power Take Off (PTO) mechanism once the OWC is used as wave energy converter (e.g. Anand et al., 2007).

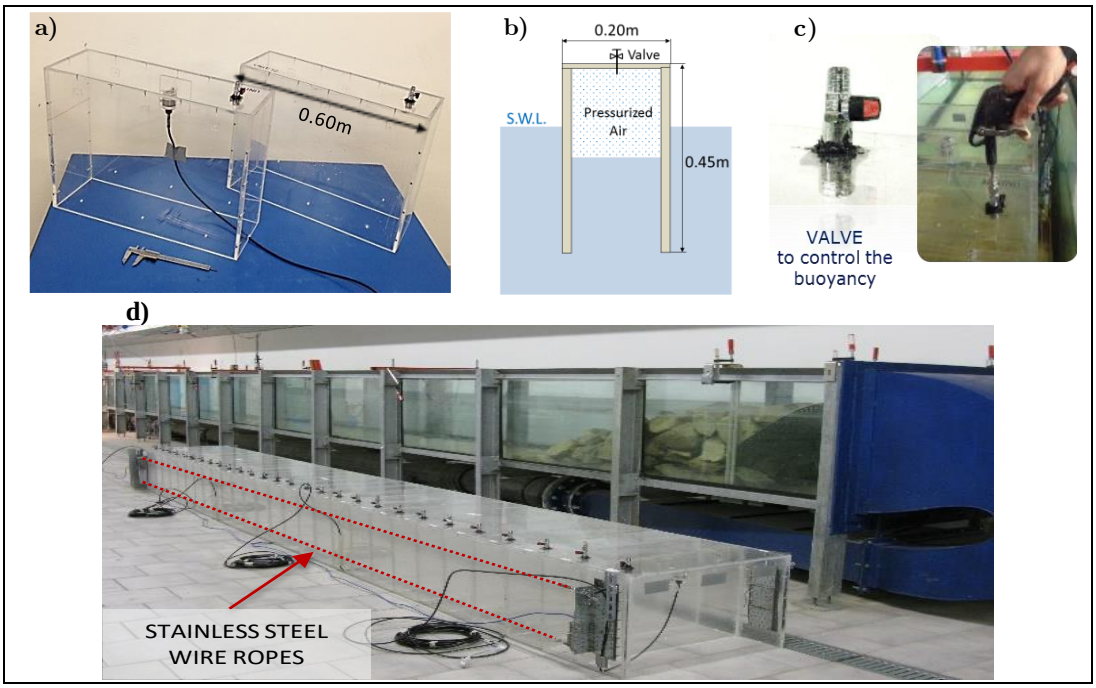

Fig. 1. VLFS model (a) Methacrylate box units composing the VLFS; (b) Side view of one semi-submerged box unit; (c) Valve equipping each box unit for buoyancy control d) Stainless steel wire ropes (red colour) used to assemble the VLFS model.

The VLFS was equipped with six OWCs, three installed in the leading edge and three in the back edge (Fig.2).

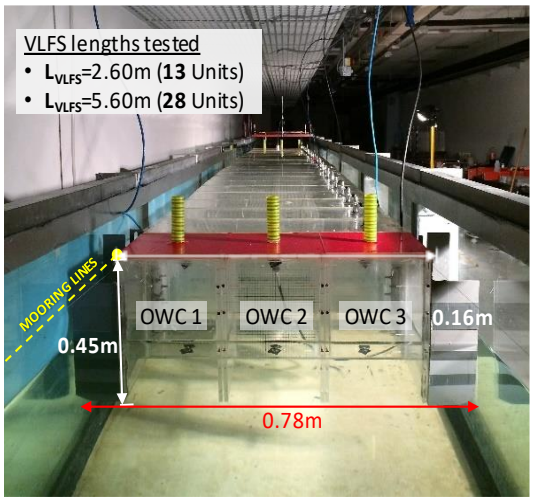

Fig. 2. Picture of the VLFS-OWCs model tested in the wave-flume.

Parameter study on the VLFS-OWC models

Considering the strong influence on OWC performance of resonance frequency (Evans, 1978), air volume (Lovas, 2010) and wave period (Sheng, 2012), and the important effect of the VLFS length in the floating response of the platform, a

parameter study assessing the effect of several design alternatives under regular and irregular waves, was carried out.

The parameter study investigated different OWC chamber widths, W (along the direction of wave propagation), front wall draughts, D, orifice area, V, and lengths of the VLFS, L_{VLFS} (Fig. 3). Two lengths of the VLFS were tested (2.6m and 5.6m) and the six most performant OWC models studied by Crema et al. (2015) were tested (Fig.3). These OWC models have the following characteristics:

- Same front wall draught, D1=-0.09m S.W.L.;
- Three different chamber widths, W1=0.10m, W2=0.20m and W3=0.30m;
- Two different orifice areas, V1% and V2% of the top cover area.

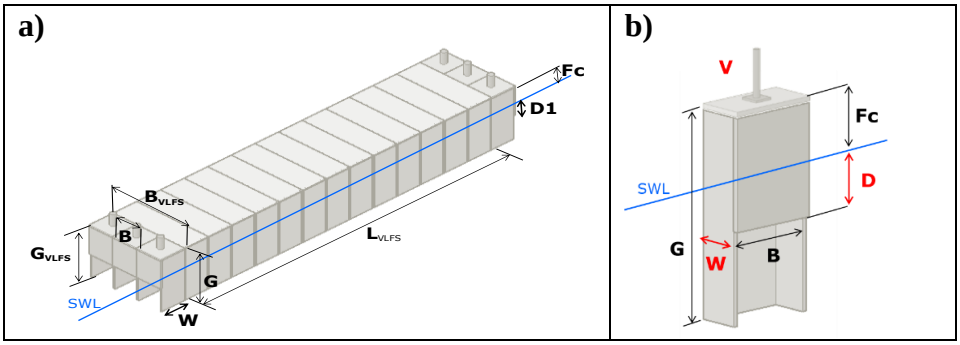

Fig. 3. Schematic view of a) the VLFS-OWC model and b) the OWC model.

Hydrodynamic test conditions

The sea states, simulated during the experimental tests, are representative of the hypothetical installation sea site located in front of the Tuscany coast (North Mediterranean Sea), as characterized by Vannucchi and Cappietti, (2013), where the water depth is 25m and the yearly mean wave energy is about 3 kW/m. Overall, the eleven different sea states in Table 1 were tested.

Table 1. Target wave parameters of the selected wave attacks (model scale 1:50)

WAVE TYPE	WAVE CODE	H [m]	T [s]
Regular	H01	0.04	0.80
Regular	H02	0.04	1.00
Regular	H03	0.04	1.40
Regular	H04	0.04	1.20
Regular	H05	0.06	0.90
Regular	H06	0.06	1.60
WAVE TYPE	WAVE CODE	Hm0 [m]	Te [s]
Irregular	H1	0.02	0.87
Irregular	H2	0.02	0.95
Irregular	H3	0.04	0.96
Irregular	H4	0.04	1.06
Irregular	H5	0.06	1.07

Experimental set-up

The experiments were carried out in the wave-current flume of the LABIMA - Laboratory of Maritime Engineering (www.labima.unifi.it) of the Civil and Environmental Engineering Department of Florence University.

The wave-current flume is 37.0m long and 0.80m wide and high. The piston type wave maker can generate random sea with a given target spectrum and maximum wave height H=0.35m for 1.0s<T<2.0s on a water depth up to 0.60m.

In this work the water depth was h=0.50m, the freeboard of the WLFS was 0.16m above the S.W.L and a passive wave absorbing system was built at the end of the flume.

The VLFS-OWC model was placed 22m far from the wave maker and was kept on site by means of four long horizontal mooring lines (two connected to the leading edge and two to the back edge), to force the movements of the VLFS as heave motion only. The mooring lines cables were made of a thin and high stiffness cotton rope and were 5.0m long, to reduce as much as possible the vertical mooring components acting on the model during the tests (Fig. 4).

Ten ultrasonic distance sensors, characterized by a declared repeatability of 1mm, were deployed along the wave flume. These sensors were used as wave gauges (WG) and as displacement meters (DM) to record the vertical motions of the VLFS model in particular:

- WG1, located in front of the wavemaker for measuring the generated waves;
- WG2 -WG4, set in front the model for measuring the incident and reflected waves
- WG11 behind the model for measuring the transmitted waves.
- WG5, installed inside the OWC to measure the internal free surface oscillations
- DM6 -DM10 were located above the model deck to measure the heave motions of 5 points along the VLFS.

Five pressure transducers, with full scale range 100mbar and accuracy of ± 0.1% FS were installed in the VLFS model and in the OWC as follows:

- PT1-PT4, inside four units of the VLFS model, to register the air pressure variations during the tests;
- PT, was located inside the OWC, to measure the pressure drop.

Only the central OWC of the three positioned in the leading and back VLFS edges, was instrumented. For a first test series, the central OWC on the leading edge was instrumented, while the central OWC on the back edge was instrumented during a repetition of the test.

One constant temperature Hot Wire anemometer (HW), with a platinum plated tungsten wire with a diameter of 5μm and a length of 1.25mm, was ad hoc calibrated in the range of 0-15m/s and installed in the duct connecting the orifice, to measure the flow rate of inlet and outlet airflow.

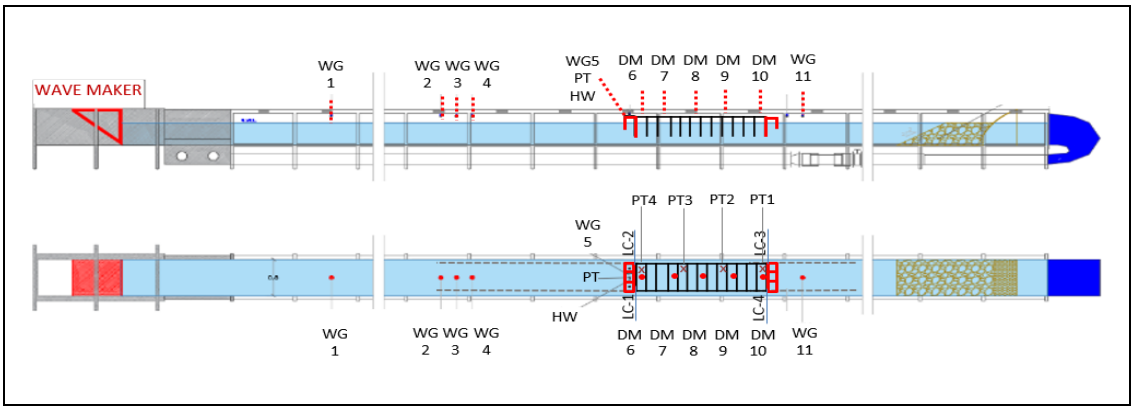

Fig. 4. Location of the model and the instruments for the tests performed on the VLFS-OWC in the wave- current flume LABIMA.

RESULTS

Energy absorbed by the OWCs integrated in the VLFS

A commonly used indicator of the performance of a Wave Energy Converter is the so-called *Capture Width*, *CW* [m], defined as the width of the wave front that contains the same amount of power as that absorbed by the device (Price et al., 2009).

The capture width, CW [m] is therefore described as the ratio of the absorbed pneumatic power, Π_{OWC}, [W] to the wave power per unit length of the wave crest of the incident waves, Π_{wave}, [W/m] (Eq.1):

$$CW = \frac{\overline{\Pi_{owc}}}{\overline{\Pi_w}} \tag{1}$$

The mean absorbed pneumatic power is obtained through integration over the test duration Ttest of the product of air pressure p(t)measured inside the OWC chamber and airflow rate Q(t) through the pipe, (Sarmento, 1993), (Eq.2):

$$\overline{\Pi_{OWC}} = \frac{1}{T_{test}} \int_0^{T_{test}} Q(t)p(t)dt \tag{2}$$

while, the period averaged wave power per unit length of the wave crest is computed for incident regular and irregular wave trains according to Cornett, (2008).

For *regular waves*, the period-averaged wave power for a specific water depth *h*, is defined according to linear wave theory by Eq. 3:

$$\overline{\Pi_{wave\ reg}} = \frac{1}{16}\rho g H^2 \frac{\omega}{k}\left(1 + \frac{2kh}{\sinh(2kh)}\right) \tag{3}$$

in which, ρ is the water density, H is the regular wave height, ω is the wave frequency and k is the wave number.

For *irregular waves*, the period-averaged wave power is calculated as:

$$\overline{\Pi_{wave\ irr}} = \rho g \sum_i c_{g,i} S_i \Delta f_i \tag{4}$$

where S_i is the frequency spectrum recorded in the laboratory tests, Δf_i is the frequency resolution and $c_{g,i}$ is the wave group celerity for each spectral wave component *i*, obtained by solving the linear dispersion relation for the specific water depth *h* (Eq. 5).

$$c_{g,i} = \frac{1}{2}\left(1 + \frac{2k_i h}{\sinh(2k_i h)}\right)\frac{g}{\omega_i}\tanh(k_i h) \quad (5)$$

in which, k_i is the wave number for component *i* and ω_i is the angular wave frequency for component *i*.

The *Relative Capture Width, CW* [-]*, is then obtained by normalizing the *Capture Width, CW*, by the OWC chamber length, *B*, which for all the tests was fixed at 0.20m:

$$CW^* = CW/B \quad (6)$$

The results obtained for the performance of a floating OWC (integrated in a VLFS) tested under regular and irregular waves, are documented in Table 2 for the VLFS 5.6m long.

Table 2. Relative Capture Width [-] assessed for each OWC alternative integrated in the VLFS (L_{VLFS}=5.6m).

WAVE CODE	OWC geometry integrated in the VLFS (L_{VLFS}=5.6m)					
	W1D1V1%	**W1D1V2%**	**W2D1V1%**	**W2D1V2%**	**W3D1V1%**	**W3D1V2%**
H01	0.25	0.37	0.44	0.30	0.29	0.14
H02	0.26	0.35	0.58	0.65	0.53	0.52
H03	0.12	0.08	0.29	0.18	0.31	0.22
H04	0.24	0.23	0.54	0.49	0.50	0.51
H05	0.25	0.40	0.52	0.52	0.46	0.39
H06	0.10	0.06	0.32	0.19	0.30	0.22
H1	0.36	0.45	0.78	0.69	0.66	0.48
H2	0.31	0.36	0.71	0.69	0.64	0.56
H3	0.37	0.46	0.77	0.80	0.72	0.69
H4	0.32	0.35	0.71	0.71	0.70	0.72
H5	0.29	0.35	0.61	0.68	0.60	0.65

In the regular wave tests, the OWC performance reaches a maximum value of 0.65, corresponding to the configurations W2D1V2% for the incident wave H02 (H=0.04m, T=1.0s). The case of chamber width W2 shows, for all wave conditions and orifice area, the highest capture width (more than 30%) for 9/12 of the tests. Generally, as observed for fixed OWC (Crema et al. 2015), the maximum efficiency is related to the wave period T=1.0s. For the medium and larger chamber widths tested (i.e., W2 and W3), increasing the orifice area from V1% to V2% (i.e. mimic the decreasing of the turbine damping), results in a decrease of the performance of the OWC integrated in the VLFS for most of the considered range of incident waves (4/6).

In the irregular wave tests the capture width reaches the maximum value of about 0.80, corresponding to the configuration W2D1V2% for the case H3 (H_{m0}=0.04m, T_p= 0.95s), related to a peak period similar as for the regular wave case. The medium

chamber width, W2, shows always the highest capture width for all the incident waves and orifice size. Smaller applied damping (V2% code) generally results in an increase of the performance for smaller chamber width (W1). For the medium chamber width (W2) and the larger one (W3), the dependence of the OWC performance by this parameter is less evident since lowering the applied damping leads to a lower capture width in 5/10 of the tests and vice versa for the remaining 5/10.

Effect of OWCs in the floating behaviour of the VLFS

At first, the influence of the VLFS length on the floating behaviour of the platform not equipped with OWCs is assessed for the two lengths: L_{VLFS}=2.6m and L_{VLFS}=5.6m, (Fig.6).

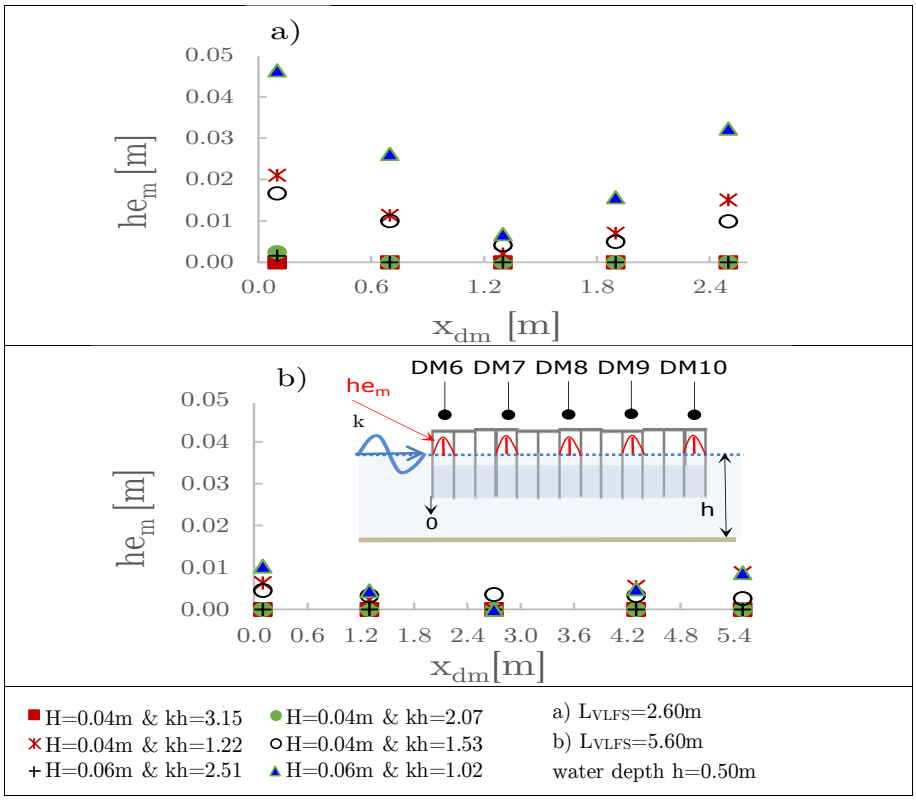

Fig. 6. Longitudinal distributions of the heave motion amplitudes he_m, for the two VLFS models not equipped with OWCs. a) L_{VLFS}=2.60m and b) L_{VLFS}=5.60m, under regular waves (x_{dm} is the distance measured from the leading edge of the VLFS).

The results show that, for both tested VLFS lengths, the maximum heave motion (he_m) always occurs at the leading edge (i.e. measured at the DM6 sensor position). For fixed wave heights, the heave motion amplitude generally increases with increasing the wave period (i.e. decreasing the relative water depth, kh, from 3.15 to 1.02).

The comparison between the two tested VLFS lengths shows that also this design parameter has a relevant effect on the VLFS floating behaviour, leading to an increase of the motion amplitude with decreasing the VLFS length. In case of L_{VLFS}=2.6m (Fig. 6a), the maximum he_m value is close to 0.05m and occurs at the leading edge (for

incident wave with H=0.06m, T=1.6s), whereas for the L_{VLFS}=5.6m (Fig. 6b), under the same wave conditions, the maximum he_m is about 5 times lower (i.e. 0.01m).

To highlight the attenuation of the VLFS floating response, due to the integration of OWC devices, the heave motion amplitudes recorded at the leading edge for the cases of VLFS without OWCs are compared with those recorded for the same VLFS equipped with all the OWC alternatives tested (Fig. 7).

As observed in He et al. (2012) and He et al. (2013) for floating breakwaters, also for VLFSs the integration of OWC devices leads to the reduction of the wave transmission on the back edge of the VLFS and the reduction of its floating motion. According to He et al. (2013) with very short waves, the heave response becomes small and the VLFS breakwater behaves like a fixed structure. Our experimental results show that the effectiveness of OWCs in attenuating the VLFS motion increases with increasing the wavelength, λ. In fact, in case of the longest waves tested, the attenuation of the motion of the leading edge assured by the OWCs reaches the considerable value of about 50%.

Moreover, for fixed wavelength, the attenuation depends also by the OWCs geometry, showing a strong dependency on the induced damping (V%) and chamber width (W), which, as observed for fixed OWC, influences the system frequency response as well as the conversion efficiency (Crema et al., 2015).

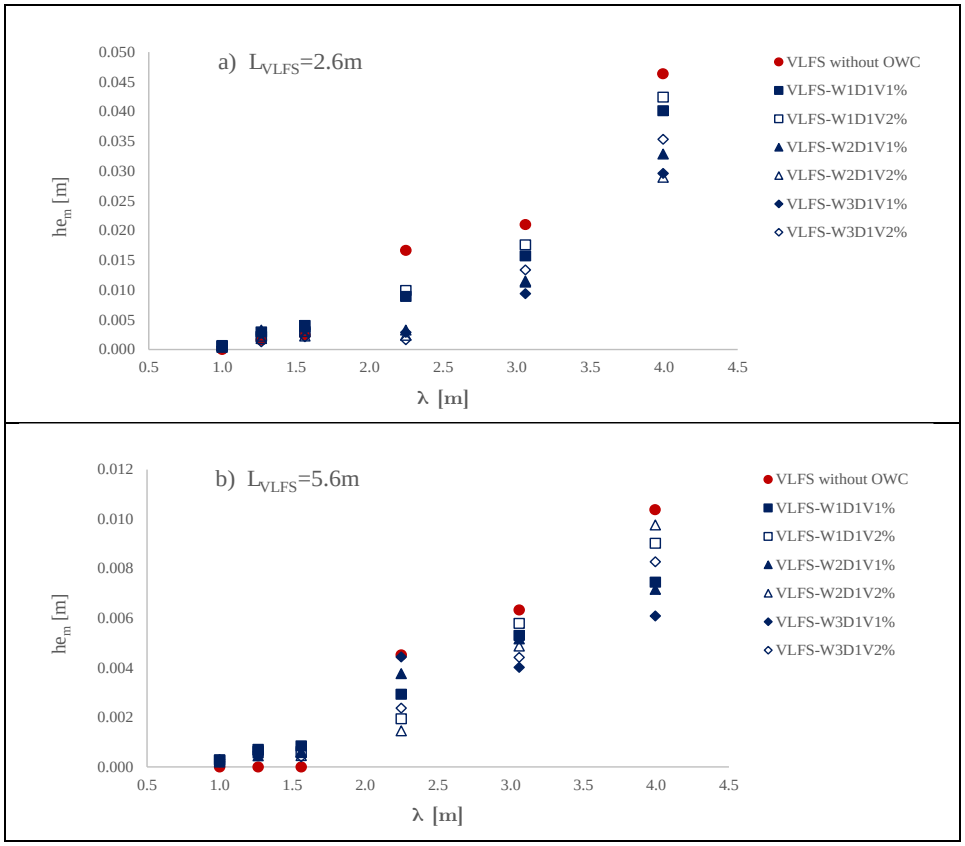

Fig. 7. Heave motion amplitudes (he_m), recorded at the leading edge, as function of the wave length, λ. a) VLFS model 2.60m long. b) VLFS model 5.6m long. Regular wave tests.

The variations of heave Response Amplitude Operators, RAOs, (i.e., he_m/a_i, where a_i is the incident wave amplitude) versus W/λ (i.e. W is the chamber width and λ is the wave length), for the VLFS 5.6m long with OWCs having the same applied damping (V1%), are reported in Fig. 8 where, the dimensionless variables suggested in He et al. (2013), are used.

This analysis was done in order to locate our experimental results within the existing literature and the deeper result analysis and discussion are post pone to future works.

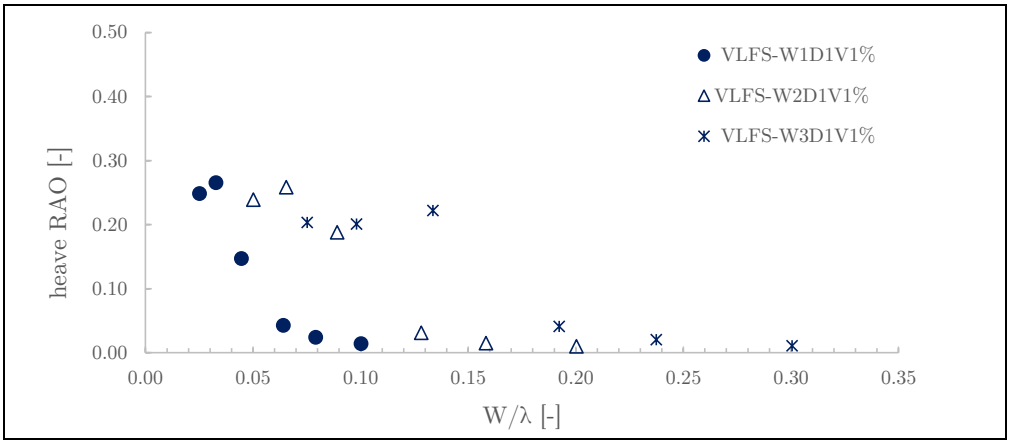

Fig. 8. Variations of heave RAOs versus W/λ for the OWCs integrated in the longest VLFS (L_{VLFS}=5.60m) with the same applied damping (V1%).

In fact, our results confirm that, for a given OWC chamber width, *W*, the heave RAOs decrease with increasing W/λ, i.e. for lower wave frequencies. Moreover, the maximum value of the heave RAO is located at a frequency value that is still a function of the chamber width thus suggesting its influence on the natural frequency of the WLFS-OWC system.

Key Words

Very Large Floating Structures, Oscillating Water Column Devices, Small-scale laboratory experiments, Parameter Study, Floating motion attenuation, Wave-energy extraction.

CONCLUSIONS

In this work, the experimental methodology and preliminary analysis aimed at assessing the effectiveness of OWCs integrated in a VLFS in attenuation its floating motion, were presented. The tested waves were representative of a specific moderated wave climate in a Mediterranean area. The VLFS model was constrained to move in the heave motion only. Increasing the length of the VLFS the heave motion strongly decreases. The motion attenuation effects, due to the integration of OWC, is always effective and is higher in case of longer wave attacks. The maximum amplitude of the heave motion along the VLFS is located to the leading edge. Up to 50% of decrement of the leading edge VLFS motion amplitude was measured. Moreover, also the pressure drops induced by the orifice on the top of the OWC and the width of the OWC (along the wave propagation direction) play a role on the effectiveness of the

motion attenuation effect. The latter seems also to play a role in the natural frequency of the VLFS-OWC system.

ACKNOWLEDGMENTS

The support of Civil and Environmental Engineering Department of Florence University under the NEMO project and the EU-H2020 MARINET2 project under the LABIMA-UNIFI partner are gratefully acknowledged.

REFERENCES

Anand, S., Jayashankar, V., Nagata, S., Toyota, K., Takao, M., & Setoguchi, T. (2007). *Performance estimation of bi-directional turbines in wave energy plants*. Journal of Thermal Science, 16(4), 346-352.

Boccotti, P. (2003). *On a new wave energy absorber.* OCEAN ENG. 30. 1191-1200. 10.1016/S0029-8018(02)00102-6.

Cornett, A.M. (2008). A global wave energy resource assessment. The Eighteenth International Offshore and Polar Engineering Conference. International Society of Offshore and Polar Engineers, 8, pp.318–326.

Crema, I., Cappietti, L., Oumeraci, H. (2015). *Laboratory Experiments on Oscillating Water Column Wave Energy Converters.* Proceedings of SCACR15, 7th International Short Conference on Applied Coastal Research, Università di Firenze (UniFI) Italy, ISBN: 978-88-97181-52-1, pp. 197-208.

Evans D. (1978). *The Oscillating Water Column Wave-energy Device*. J. Inst. Maths Applies, 423-433.

Falcão, A.F. de O. (2010). *Wave energy utilization: A review of the technologies.* Renewable and Sustainable Energy Re-views 14: 899-918.

He, F., Huang, Z. & Law, A.W.-K. (2013). *An experimental study of a floating breakwater with asymmetric pneumatic chambers for wave energy extraction*. Applied Energy, 106, pp.222–231.

He, F., Huang, Z. & Wing-Keung Law, A. (2012). *Hydrodynamic performance of a rectangular floating breakwater with and without pneumatic chambers: An experimental study*. Ocean Engineering, 51, pp.16–27.

Hong, S. Y., and Kyoung, J. H. (2006). *Hydroelastic Response of VLFS Coupled With OWC-Type Breakwater*. Proceedings of the Fourth International Conference on Hydroelasticity in Marine Technology, Wuxi, China, pp. 245–254.

Hong, S. Y., and Kyoung, J. H. (2007). *Effects of Location and Shape of OWC-Chamber on the Hydroelastic Response of VLFS*. Proceedings of the 7th International Offshore and Polar Engineering Conference, Lisbon, Portugal, pp. 434–438.

Hong, S. Y., Kim, B. W., and Kyoung, J. H. (2009). *Numerical and Experimental Study on Coupled Hydroelastic Behaviour of VLFS and OWC Chamber*. Proceedings of the 5th International Conference on Hydroelasticity in Marine Technology, Southampton, UK, pp. 303–312.

Hughes, S.A. (1993). *Physical Models and Laboratory Techniques in Coastal Engineering* Vol. 7. World Scientific.

Ikoma, T., Maeda, H., Masuda, K., and Rheem, C.-K. (2003). *Effects of the Air-Chambers on the Hydroelastic Response Reduction.* Proceedings of International Symposium on Ocean Space Utilization Technology, Tokyo, Japan, pp. 180–188.

Lovas S. (2010). *Theoretical modeling of two wave-power devices*. Master Thesis, Department of Civil and Environmental Engineering MIT.

Maeda, H., Onishi, Y., Rheem, C.-K., Ikoma, T., Washio, Y., Osawa, H., and Arita, M. (2000). *Flexible Response Reduction on a Very Large Floating Structure due to OWC Wave Power Devices*. J. Soc. Nav. Archit. Jpn., 188, pp. 279–285.

Maeda, H., Rheem, C.-K., Washio, Y., Osawa, H., Nagata, Y., Ikoma, T., Fujita, N., and Arita, M. (2001). *Reduction Effects of Hydroelastic Responses on a Very Large Floating Structure With Wave Energy Absorption Devices Using OWC System.* ASME Paper No. OMAE2001/OSU-5013.

Price, A. A. E., Dent, C. J., & Wallace, A.R. (2009). *On the capture width of wave energy converters*. Applied Ocean Research, 31(4), 251-259. Applied Ocean Research, 31(4), pp.251–259.

Sarmento A. (1993). *Model-Test Optimization of an OWC Wave Power Plant*, International Journal of Offshore and Polar Engineering, pp. 62-62.

Sheng W., Lewis T., Alcorn R. (2012). *On wave energy extraction of oscillating water column device*. ICOE, Dublin.

Shigemitsu, H., Ogata, T., Kobayashi, H., Inoue, K.-I., Fukuoka, T., and Takaoki, T. (2001). *Feasibility Study of Reducing Wave Load on Pontoon-Type Mega-Float Structure*. ASME Paper No. OMAE2001/OSU-5011.

Vannucchi V., Cappietti L. (2013). *Wave Energy Estimation In Four Italian Nearshore Areas*, Proceedings of the ASME 2013, 32nd International Conference on Ocean, Offshore and Arctic Engineering OMAE2013 June 9-14, Nantes, France.

Wang, C. M., Tay, Z. Y., Takagi, K., & Utsunomiya, T. (2010). *Literature review of methods for mitigating hydroelastic response of VLFS under wave action.* Applied Mechanics Reviews, 63(3), 030802.

Wang, C. M., Tay, Z. Y. (20111). *Very Large Floating Structures: Applications, Research and Development*, Procedia Engineering, Volume 14, 2011, Pages 62-72, ISSN 1877-7058.